

A COMPARATIVE PERFORMANCE EVALUATION OF NEURAL NETWORK ALGORITHMS BASED STATE OF CHARGE ESTIMATION FOR LITHIUM-ION BATTERY

M.S.H. Lipu¹, A. Ayob¹, A. Hussain¹, M.A. Hannan²
and M.A. Salam³

¹Faculty of Engineering and Built Environment,
Universiti Kebangsaan Malaysia, 43600
Bangi, Selangor, Malaysia.

²College of Engineering,
Universiti Tenaga Nasional, 43000
Kajang, Selangor, Malaysia.

³Faculty of Engineering,
Western University, N6A 5B9
Ontario, Canada.

Corresponding Author's Email: lipu@ukm.edu.my

Article History: Received 17 December 2019; Revised 7 April 2020;
Accepted 17 July 2020

ABSTRACT: This work presents a comparative analysis of state of charge (SOC) estimation for lithium-ion battery using neural network algorithms. The lithium-ion battery has been operating successfully in the automotive industry due to the long-life cycles, low memory effect, high voltage, and high energy density. As such, numerous research works have been conducted on lithium-ion battery towards estimating SOC. The conventional and model-based SOC estimation approaches have shortcomings including heavy computational calculation and inaccurate battery model parameters determination. Therefore, neural network algorithms based SOC estimation have received huge attention since they have the adaptively to adjust the network parameters automatically without battery model. Three prominent neural network algorithms including backpropagation neural network (BPNN), radial basis function neural network (RBFNN) and recurrent nonlinear autoregressive with exogenous inputs neural network (RNARXNN) are used to compare the SOC estimation results. The three methods are validated by battery experimental tests and electric vehicle (EV) drive cycles. The results demonstrate that RNARXNN is dominant to BPNN and RBFNN algorithms in obtaining high SOC accuracy with the low computational cost.

KEYWORDS: *State of Charge; Lithium-ion Battery; Neural Network; Electric Vehicle; Drive Cycles*

1.0 INTRODUCTION

The demand for battery storage systems (BSSs) is increasing at a dramatic rate around the world to address carbon emissions, climate change, and global warming challenges [1]. The global battery market is growing rapidly especially in Asia-Pacific regions with government incentives, supportive policies, and regulations which in turn generates huge revenue to the battery industries. Several electrochemical rechargeable batteries are being actively used in different applications [2]. The lithium-ion battery holds promising features in terms of high energy capacity, high voltage and long lifecycle [3].

State of charge (SOC) indicates the existing charge capacity which is stored inside a lithium-ion battery [4]. Various SOC estimation algorithms have been reported in the literature [5]. Generally, SOC estimation methods are classified into three groups; conventional approach, model-based approach, and intelligent approach. The coulomb counting method and open-circuit voltage (OCV) are known as conventional approaches. The coulomb counting method has a simple execution but suffers from poor robustness and accumulator error [6]. The OCV method has reasonable precision but has a limitation of online implementation [7]. Kalman filter (KF) is commonly used as model-based SOC estimation techniques [8]. They can deliver accurate results; however, their execution is constrained by highly complex mathematical computation and inaccurate battery model parameters. Fuzzy logic and neural network are the popular subclasses of intelligent approaches. Fuzzy logic offers good results; however, the generation of fuzzy rules is a difficult task due to battery non-linear characteristics [9].

The neural network algorithms offer excellent outcomes in SOC estimation since they do not need an added filter, battery model, extensive mathematical equations to capture the battery non-linear characteristics. Hence, this paper presents the comparative analysis of SOC estimation for lithium-ion battery using state-of-the-art neural network algorithms including backpropagation neural network (BPNN), radial basis function neural network (RBFNN), and recurrent non-linear auto-regressive with exogenous inputs neural network (RNARXNN) algorithms.

The performance is compared using different error rate terms and computational cost.

2.0 NEURAL NETWORK ALGORITHMS BASED SOC ESTIMATION METHODS

2.1 BPNN Algorithm

A feed-forward BPNN model is designed using three layers; input layer, hidden layer, and output layer, as shown in Figure 1 [10].

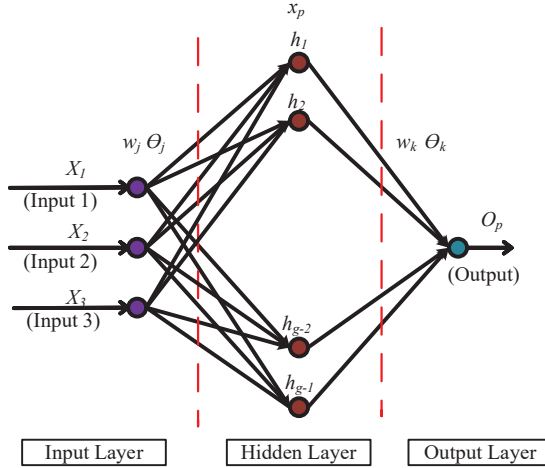


Figure 1: BPNN structure for SOC estimation

The hidden layer output is expressed using the following equations [11]:

$$O_j = f(\text{net}_j) \quad (1)$$

$$\text{net}_j = \sum_j w_{i,j} x_i + \theta_{i,j} \quad (2)$$

$$f(\text{net}) = \frac{1}{1 + e^{-(\text{net})}} \quad (3)$$

where, $w_{i,j}$ and $\theta_{i,j}$ denote the weight and bias from the input layer to the hidden layer. The operation of the hidden layer is performed using the log-sigmoid transfer function. The final result of the output layer as shown in [11]] can be written such as

$$O_k = f(\text{net}_k) \quad (4)$$

$$\text{net}_k = \sum_k w_{j,k} O_j + \theta_{j,k} \quad (5)$$

The weight and bias from the hidden layer to the output layer is denoted as $w_{k,j}$ and $\theta_{k,j}$ respectively. The output layer uses a linear activation function to deliver the results. The output layer error is calculated as

$$e_k = T_k - O_k \tag{6}$$

$$\partial_k = e_k f'(net_k) \tag{7}$$

The true output is denoted as T_k . The hidden layer error can be formulated as

$$\partial_j = f'(net_j) \partial_k w_{j,k} \tag{8}$$

The value of weight and biases are updated using the following equations [11]:

$$\Delta w_{j,k} = \alpha \partial_k O_j \tag{9}$$

$$w_{j,k} = w_{j,k} + \Delta w_{j,k} \tag{10}$$

$$\Delta w_{i,j} = \alpha \partial_k x_i \tag{11}$$

$$w_{i,j} = w_{i,j} + \Delta w_{i,j} \tag{12}$$

$$\Delta \theta_{j,k} = \alpha \partial_k \tag{13}$$

$$\theta_{j,k} = \theta_{j,k} + \Delta \theta_{j,k} \tag{14}$$

$$\Delta \theta_{i,j} = \alpha \partial_j \tag{15}$$

$$\theta_{i,j} = \theta_{i,j} + \Delta \theta_{i,j} \tag{16}$$

where α is the learning rate.

2.2 RBFNN Algorithm

A RBFNN is a feed-forward self-learning algorithm that consists of a non-linear function with a symmetrical organization. The structure of RBFNN consists of three-layer including one input layer, one hidden layer and one output layer as shown in Figure 2. The center and width terms of the j Gaussian distribution function are denoted by λ_m and σ_m , respectively [12]. The output of the m th hidden neuron of the RBFNN can be expressed as in [12] such as

$$\begin{aligned} \phi_m(n) &= \phi_m \{x(n), \lambda_m(n), \sigma_m(n)\} \\ &= e^{-\frac{\|x(n) - \lambda_m(n)\|^2}{\sigma_m^2(n)}}, \text{for } m=1,2,\dots,M \end{aligned} \tag{17}$$

where, x is the input vector in the input layer, λ_m and σ_m represent the center and width of m^{th} hidden neurons in the Gaussian function, respectively. The output of RBFNN comprises linear function and is determined by multiplying the weight values with hidden nodes, as shown in the following equation [12]:

$$y_k = \sum_{m=1}^M w_{km} \phi_m(n), \text{ for } k = 1, 2, \dots, m \quad (18)$$

where, y_k represents the output of the k^{th} neuron in the output layer, w_{km} denotes the weight that connects the m^{th} hidden neurons to the k^{th} output layer neuron and ϕ_m is the hidden layer output for m^{th} neurons.

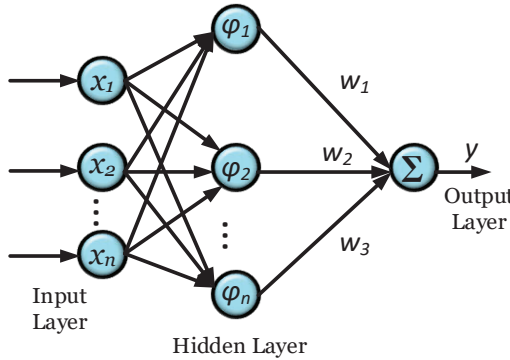


Figure 2: The structure of RBFNN for SOC estimation

2.3 RNARXNN Algorithm

RNARXNN algorithm exhibits improved learning performance and fast computational speed which is suitable to address lithium-ion battery non-linear characteristics. The structure of RNARXNN is configured using three layers like BPNN and RBFNN and additional output feedback layer and past information of the input layer, as shown in Figure 3 [13]. In this paper, the SOC estimation is estimated using a parallel architecture based RNARXNN method where the training and validation processes are operated using the closed-loop system. The output of RNARXNN can be formulated as in [13] such

$$y(n+1) = f_0 \left[b_0 + \sum_{h=1}^N w_{h0} \cdot f_h \left(b_h + \sum_{i_1=0}^{du_1} w_{i_1 h} u_1(n-i_1) + \sum_{i_2=0}^{du_2} w_{i_2 h} u_2(n-i_2) + \sum_{j=0}^{dy} w_{jh} y(n-j) \right) \right] \quad (19)$$

where weights, biases, and activation functions are characterized by $w_{ih}, w_{ho}, w_{jh}; b_0, b_h; f_h(\cdot)$, and $f_0(\cdot)$, respectively. The hidden layer and output layer operation is implemented using log-sigmoid and purelin transfer function, respectively.

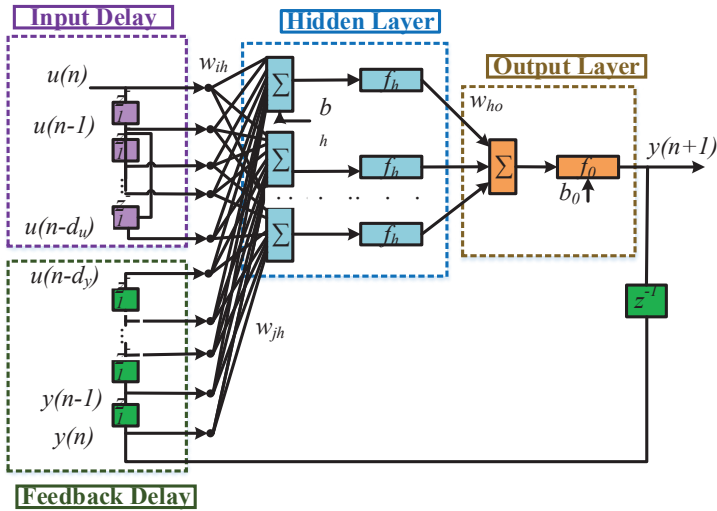


Figure 3: RNARXNN design for SOC estimation

3.0 LITHIUM-ION BATTERY EXPERIMENTS AND DATA DEVELOPMENT

The experimental tests are conducted using NCR18650B lithium-ion batteries developed by Panasonic. Table 1 shows the specification of the Panasonic NCR18650B lithium-ion battery cell.

Table 1: Specifications of LiNiCoAlO₂ battery

Type	Nominal capacity (mAh)	Nominal voltage (V)	Cut-off voltage min/max (V)	Specific Energy (Wh/kg)	Cycle life
LiNCA	3200	3.60	2.5/4.2	200-260	500

3.1 Experimental Configuration

A lithium-ion battery test bench model is developed which is divided into two parts, namely hardware part and software part, as displayed in Figure 4. The hardware part comprises a LiNiCoAlO₂ battery and NEWARE BTS-4000. The software part includes BTS software version 7.6 and MATLAB 2015a which are installed on the host computer. The control unit of NEWARE BTS-4000 is connected to a host computer through TCP/IP Port while BTS-4000 measurement unit is connected to the control unit through RS485 port.

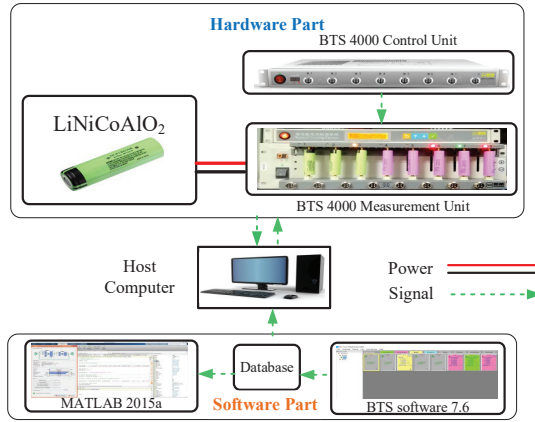


Figure 4: Lithium-ion battery test bench model configuration

3.2 Hybrid Pulse Power Characterization (HPPC) Test, DST and FUDS Drive Cycle

HPPC test is a combination of sequence charge and discharge current pulses. The procedures of HPPC can be found in [14]. SOC is further evaluated using two commonly used EV drive cycles including dynamic stress test (DST), and federal urban drive schedule (FUDS). The complete duration of one drive cycle for DST, and FUDS cycles is estimated to be 360 s, and 1372 s, respectively [15].

4.0 SOC DATA PREPARATION AND PERFORMANCE ASSESSMENT INDICATORS

After the algorithm development followed by the experimental data measurements, the whole dataset is separated into two subdivisions. The neural network-based SOC methods are trained using 70% data while the leftover unseen 30% data is used for SOC testing. Before the data training operation begins as referred in [11], data normalization is executed using the limit of [-1, 1] as shown in Equation (20) such as

$$x = \frac{2(x - x_{\min})}{x_{\max} - x_{\min}} - 1 \quad (20)$$

The maximum number of epochs during the training stage is set to be 1000. The performance goal is fixed to be 0.000001. The proposed method is validated using numerous performance indicator terms as shown in Equations (21)-(26) [16].

$$SOC\ error = SOC_a - SOC_{es} \quad (21)$$

$$RMSE = \sqrt{\frac{1}{N} \sum_{i=1}^N (SOC_{a_i} - SOC_{es_i})^2} \quad (22)$$

$$MSE = \frac{1}{N} \sum_{i=1}^N (SOC_{a_i} - SOC_{es_i})^2 \quad (23)$$

$$MAE = \frac{1}{N} \sum_{i=1}^N (SOC_{a_i} - SOC_{es_i}) \quad (24)$$

$$MAPE = \frac{1}{N} \sum_{i=1}^N \left| \frac{SOC_{a_i} - SOC_{es_i}}{SOC_{a_i}} \right| \quad (25)$$

$$SD = \sqrt{\frac{1}{N-1} \sum_{i=1}^N (SOC_{error} - \overline{SOC_{error}})^2} \quad (26)$$

where RMSE, MSE, MAE, MAPE and SD stand for root mean squared error, mean squared error, mean absolute error, mean absolute percentage error, and standard deviation, respectively. SOC_a , SOC_{es} and $\overline{SOC_{error}}$ denote the reference SOC value, estimated SOC value and average SOC error (SE), respectively.

5.0 EXPERIMENTAL VERIFICATION AND PERFORMANCE COMPARISON

SOC and SE calculation results are verified under three different cases. The first case is related to HPPC load profiles while the second and third cases are associated with the EV drive cycles including DST and FUDS. The experimental results for HPPC load profiles are illustrated in Figure 5. It is noticed that the difference between the SOC estimated by RNARXNN method and reference SOC is very small while SOC determined by BPNN and RBFNN approaches is not aligned with the reference SOC. There is a drop of 61.2%, and 63.2% in RNARXNN method in comparison to BPNN, and RBFNN methods, respectively while assessing SD as shown in Table 2.

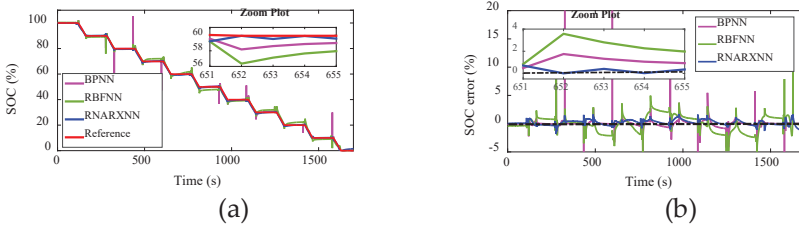


Figure 5: Lithium-ion battery SOC performance in case 1 under HPPC test: (a) SOC and (b) SOC error

Table 2: SOC performance comparison in HPPC test

Method	RMSE (%)	MSE (%)	MAE (%)	MAPE (%)	SD (%)
BPNN	1.3974	0.0195	0.4685	7.288	1.3977
RBFNN	1.4744	0.0217	0.6217	10.7982	1.4748
RNARXNN	0.5554	0.0031	0.2480	5.5931	0.5413

SOC performance evaluation is also analyzed for DST drive cycle as indicated in Figure 6. The RMSE of the RNARXNN algorithm is computed to be 0.5347% which is 49.7%, and 56.6%, reduction from the BPNN, and RBFNN algorithms, respectively, as shown in Table 3. The results are also reported satisfactory in RNARXNN method towards assessing MSE, MAE, MAPE, and SD values. SOC is further tested using FUDS drive cycle as illustrated in Figure 7.

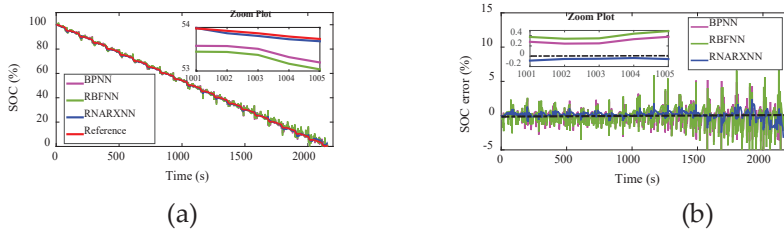


Figure 6: Lithium-ion battery SOC performance in case 2 under DST drive cycle: (a) SOC and (b) SOC error

Table 3: SOC performance comparison in DST cycle

Method	RMSE (%)	MSE (%)	MAE (%)	MAPE (%)	SD (%)
BPNN	1.0648	0.0113	0.7265	5.9903	1.0650
RBFNN	1.2329	0.0152	0.8432	16.7005	1.2332
RNARXNN	0.5347	0.0029	0.3519	4.1362	0.5259

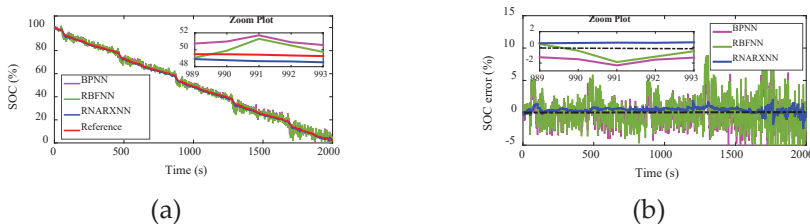


Figure 7: Lithium-ion battery SOC performance in case 3 under FUDS drive cycle: (a) SOC and (b) SOC error

It is noticed that RNARXNN method has improved performance in achieving low RMSE, MSE, MAE, MAPE, and SD. For instance, the MSE is reported high in BPNN and RBFNN algorithms, indicating 0.0414% and 0.0578%, respectively while that for RNARXNN algorithm is 0.0038%, as shown in Table 4.

Table 4: SOC performance comparison in FUDS cycle

Method	RMSE (%)	MSE (%)	MAE (%)	MAPE (%)	SD (%)
BPNN	2.0350	0.0414	1.4061	10.8794	2.0351
RBFNN	2.4044	0.0578	1.8065	13.2654	2.4049
RNARXNN	0.6188	0.0038	0.5358	3.6918	0.6192

The effectiveness of three neural network algorithms is further analyzed based on SE and computational cost (CC), as shown in Table 5. The CC comprises both training and testing duration. In case 1, SE in RNARXNN algorithm is very low and restricted under 2%. Also, CC is computed to be very low in comparison to other two methods, indicating 2.8875 s. In Case 2, The RNARXNN algorithm achieves reasonable accuracy while reducing SE under 4%. Moreover, the CC is achieved to be 3.2615 s which is smaller than BPNN, and RBFNN algorithms. In case 3, The RNARXNN method also achieves good results with SE under 4%. The results are also excellent in terms of obtaining fast estimation speed with the CC of 4.3856 s.

Table 5: SOC performance comparison in three cases

Cases	Case 1 HPPC Test		Case 2 DST Cycle		Case 3 FUDS Cycle	
	SE (%)	CC (s)	SE (%)	CC (s)	SE (%)	CC (s)
BPNN	[-10.25, 21.38]	28.5836	[-7.47, 5.19]	28.2487	[-8.42, 10.15]	29.5678
RBFNN	[-5.29, 13.81]	8.3856	[-8.48, 9.56]	10.3846	[-8.12, 11.73]	17.4557
RNARXNN	[-1.84, 1.72]	2.8875	[-3.25, 2.37]	3.2615	[-3.14, 2.13]	4.3856

The accuracy of the proposed RNARXNN method is compared with the existing model-based methods under EV drive cycles. It is reported that OCV [15], proportional integral observer (PIO) [17], and unscented particle filter (UPF) have RMSE above 1% while that for RNARXNN is below 1% [18]. The results prove that RNARXNN method is more accurate and robust than existing SOC estimation approaches.

6.0 CONCLUSION

A comparative performance assessment of SOC estimation using neural network algorithms is presented. The neural network algorithms are validated by developing a battery test bench model and HPPC experiments. Besides, the robustness of the neural network algorithms is checked under two EV drive cycles. The results demonstrate that RNARXNN achieves better results than BPNN and RBFNN methods with regard to different error indicator terms. Besides, RNARXNN obtains SOC error under 2%, 4% and 4% in Case 1, Case 2 and Case 3, respectively. Furthermore, RNARXNN computes RMSE below 1% in all three cases. Besides, the fast CC of SOC confirms

the appropriateness and implementation of RNARXNN in a real-world environment. The future work includes the temperature effect and aging cycles to assess SOC.

ACKNOWLEDGMENTS

The research work was supported by Universiti Kebangsaan Malaysia under grant LRGS/2018/UNITEN-UKM/EWS/04.

REFERENCES

- [1] A.R. Dehghani-Sanij, E. Tharumalingam, M.B. Dusseault and R. Fraser, "Study of energy storage systems and environmental challenges of batteries", *Renewable and Sustainable Energy Review*, vol. 104, no. 1, pp. 192–208, 2019.
- [2] E. Chemali, P.J. Kollmeyer, M. Preindl and A. Emadi, "State-of-charge estimation of Li-ion batteries using deep neural networks: A machine learning approach", *Journal of Power Sources*, vol. 400, no. 1, pp. 242–255, 2018.
- [3] B. Xiao, Y. Liu and B. Xiao, "Accurate state-of-charge estimation approach for lithium-ion batteries by gated recurrent unit with ensemble optimizer", *IEEE Access*, vol. 7, no. 1, pp. 54192–54202, 2019.
- [4] E. Chemali, P. Kollmeyer, M. Preindl, R. Ahmed and A. Emadi, "Long Short-Term Memory-Networks for Accurate State of Charge Estimation of Li-ion Batteries", *IEEE Transactions on Industrial Electronics*, vol. 65, no. 8, pp. 6730–6739, 2017.
- [5] R.U.I. Xiong, J. Cao and Q. Yu, "Critical Review on the Battery State of Charge Estimation Methods for Electric Vehicles", *IEEE Access*, vol. 6, no. 1, pp. 1832–1843, 2018.
- [6] K.S. Ng, C.S. Moo, Y.P. Chen and Y.C. Hsieh, "Enhanced coulomb counting method for estimating state-of-charge and state-of-health of lithium-ion batteries", *Applied Energy*, vol. 86, no. 9, pp. 1506–1511, 2009.
- [7] F. Zheng, Y. Xing, J. Jiang, B. Sun, J. Kim and M. Pecht, "Influence of different open circuit voltage tests on state of charge online estimation for lithium-ion batteries", *Applied Energy*, vol. 183, no. 1, pp. 513–525, 2016.

- [8] Y. Li, C. Wang and J. Gong, "A combination Kalman filter approach for State of Charge estimation of lithium-ion battery considering model uncertainty", *Energy*, vol. 109, no. 1, pp. 933–946, 2016.
- [9] X. Hu, S.E. Li and Y. Yang, "Advanced Machine Learning Approach for Lithium-Ion Battery State Estimation in Electric Vehicles", *IEEE Transaction on Transportation Electrification*, vol. 2, no. 2, pp. 140–149, 2016.
- [10] S. Tong, J.H. Lacap and J.W. Park, "Battery state of charge estimation using a load-classifying neural network", *Journal of Energy Storage*, vol. 7, no. 1, pp. 236–243, 2016.
- [11] W. He, N. Williard, C. Chen and M. Pecht, "State of charge estimation for Li-ion batteries using neural network modeling and unscented Kalman filter-based error cancellation", *International Journal of Electrical Power and Energy System*, vol. 62, no. 1, pp. 783–791, 2014.
- [12] W.Y. Chang, "Estimation of the state of charge for a LFP battery using a hybrid method that combines a RBF neural network, an OLS algorithm and AGA", *International Journal of Electrical Power and Energy System*, vol. 53, no. 1, pp. 603–611, 2013.
- [13] H. Chaoui and C.C. Ibe-Ekeocha, "State of Charge and State of Health Estimation for Lithium Batteries Using Recurrent Neural Networks", *IEEE Transaction on Vehicular Technology*, vol. 66, no. 10, pp. 8773–8783, 2017.
- [14] W. Li, L. Liang, W. Liu and X. Wu, "State of Charge Estimation of Lithium-Ion Batteries Using a Discrete-Time Nonlinear Observer", *IEEE Transaction on Industrial Electronics*, vol. 64, no. 11, pp. 8557–8565, 2017.
- [15] Y. Xing, W. He, M. Pecht and K.L. Tsui, "State of charge estimation of lithium-ion batteries using the open-circuit voltage at various ambient temperatures", *Applied Energy*, vol. 113, pp. 106–115, 2014.
- [16] F. Yang, X. Song, F. Xu and K.L. Tsui, "State-of-Charge Estimation of Lithium-Ion Batteries via Long Short-Term Memory Network", *IEEE Access*, vol. 7, no. 1, pp. 53792–53799, 2019.
- [17] L. Zheng, L. Zhang, J. Zhu, G. Wang and J. Jiang, "Co-estimation of state-of-charge, capacity and resistance for lithium-ion batteries based on a high-fidelity electrochemical model", *Applied Energy*, vol. 180, no. 1, pp. 424–434, 2016.
- [18] Y. He, X. Liu, C. Zhang and Z. Chen, "A new model for State-of-Charge (SOC) estimation for high-power Li-ion batteries", *Applied Energy*, vol. 101, no. 1, pp. 808–814, 2013.